

## Investigating the Performance of 5G Signals in Modeling Processing Algorithms in a Semi-Active Radar System

Sayed Sarwar Ebtekar<sup>✉1</sup>, Rajab Ali Khavari<sup>2</sup>

<sup>1,2</sup>Kabul University, Department of Clinical Pharmacy, Faculty of Pharmacy, Afghanistan

<sup>✉</sup>E-mail: [Ebtekar.sarwar@gmail.com](mailto:Ebtekar.sarwar@gmail.com), (corresponding author)

---

### ABSTRACT

The present research investigates the feasibility of utilizing standard 5G communication signals in semi-active radar systems (SARS). With the development of communication technologies, 5G signals have been considered as an illumination source for semi-active radars. With the limited expansion of 5G networks, conducting experimental studies in this field is challenging. Therefore, signal processing modeling is considered an essential solution to advance research in this field. The use of 5G signals can open new horizons in the development of high-resolution semi-active radar systems. The aim of this paper, focusing on the analysis of 5G-downlink signal characteristics and signal processing modeling in PALS, is to evaluate the capabilities and identify the system in providing high resolution in two dimensions (range and speed). To achieve the research objectives, the semi-active radar (PARL), standard, and structure (PARL) models, as well as the 5G signal propagation channel model, were based on the principles of signal processing theory. Computer modeling was used to calculate the PARL mutual uncertainty function using 5G signals. The results of the simulations showed that the semi-active radar system using 5G signals is capable of detecting targets with high resolution in both dimensions (range and speed). This system showed good performance in different scenarios. Therefore, 5G signals as an illumination source can be a suitable option for the development of PALS systems. It is suggested that, with the expansion of 5G networks, experimental studies should be conducted to validate the results of this administration is necessary to optimize withdrawal guidelines.

---

### ARTICLE INFO

#### Article history:

Received: April 19, 2025

Revised: August 6, 2025

Accepted: September 13, 2025

Published: September 30, 2025

#### Keywords:

Signals, 5G, illumination signal, mutual uncertainty function, Direct signal, noise signal, semi-active radar

---

**To cite this article:** Ebtikar, S. S. & Khavari, R. A. (2025). Investigating the performance of 5G signals in modeling processing algorithms in a semi-active radar system. *Journal of Natural Science Review*, 3(3)191-207. <https://doi.org/10.62810/jnsr.v3i3.222>

**link to this article:** <https://kujnsr.com/JNSR/article/view/222>



Copyright © 2025 Author(s). This work is licensed under a Creative Commons Attribution-NonCommercial 4.0 International License.

## INTRODUCTION

Semi-active radar using external illumination sources is one of the most active areas of research and development in the field of creating air and maritime surveillance systems (Martelli et al., 2020). In recent years, significant efforts have been made towards improving the underlying processing algorithms in terms of minimizing computational complexity and achieving efficiency (Zhenyu et al., 2022). In addition, the development of new semi-active radar systems (PARLS) is ongoing, with research focusing on utilizing emerging signal sources (Gomez & Samczynski, 2022). The development of 5G networks brings new

illumination sources to semi-active radars, according to previous evaluations and studies (Veremyev & Kutuzov, 2024). PARLS using 5G signals has a relatively limited coverage and operational area, but has high resolution in terms of range and speed. PARLS using 5G signals can be used for vehicle monitoring, especially to ensure safety in rail transport or at intersections (Blázquez-García & Markiton, 2024). This research investigates the benefits of 5G technology in enhancing the performance of semi-active radars, the impact of environmental and interference factors on detection quality, and the operational challenges associated with implementing this system.

Today, 5G communication networks are being deployed in many countries around the world, including Russia and Vietnam. The 5G standard features a flexible frequency spectrum structure, allowing countries to determine the optimal frequency range for its use. Each range has its own unique technical characteristics. This, in turn, leads to differences in studies conducted for radar stations, including the carrier frequency and bandwidth used (Qisong et al., 2011). Currently, the fifth-generation experimental network is available only in a few specific locations in certain regions, and the number of user devices supporting this communication standard is limited. In this regard, modeling is becoming one of the primary methods for evaluating PARLS capabilities using 5G signals (Feifeng et al., 2010).

Given the recent advances in 5G technology and the need for high-precision and high-performance radar systems, it is of particular importance to investigate the performance of 5G signals in signal processing algorithms in semi-active radar systems. This research examines the capabilities, challenges, and solutions of utilizing 5G signals in a semi-active radar scenario, employing the least squares method (LMS), and the simulation parameters. Modeling was performed for two possible radar scenarios: with one and two moving targets in a multi-beam environment, and an analysis of the modeling results was performed (Walter & Ronald, 1995).

This study examines the structural characteristics, and main characteristics of the 5G signal, the semi-active radar scenario, modeling parameters, and frequency least squares methods and modeling methods in two cases, has the following research questions:

1. (Focus on Performance): To what extent can using 5G downlink signals as a passive illumination source improve spatial accuracy and target detection in a PALS system under different environmental and interference conditions?
2. (Focus on Challenges): What are the most important operational obstacles and challenges in implementing a PALS system based on 5G signals, and how can they be overcome?

## **METHOD AND MATERIALS**

This research employs a computer modeling method, based on previously collected data and signal algorithms in the reference channel, as well as an adaptive filter algorithm, to investigate the performance of 5G signals in semi-active radar processing algorithms (PALS).

Given the limited access to 5G networks, simulation has been chosen as the primary tool to evaluate the capabilities of this system. In this regard, the 5G downlink signal parameters in the n79 band are simulated according to the 3GPP standard. A new propagation channel model is designed for an urban scenario with direct line-of-sight conditions, and the delay and multipath power parameters are calculated based on stochastic distributions. Here, two radar scenarios including moving targets at a range of 650 m at a speed of less than 60 km/h are simulated, and the LMS adaptive filter with a  $S_{straight}(t) = S_{echo}(t) + S_{many}(t) + \omega_{nab}(t)$  (Aleksey, B., & Evgenii, V. , 2016). An algorithm is used to remove noise and interference. Equation  $\chi(\tau, f_d) = \int_{-\infty}^{\infty} S_{nab}(t) S_{straight}^*(t - \tau) e^{-j2f_d t} dt$  which forms the core of the semi-active radar processing for range and velocity estimation, is fitted to the mutual uncertainty function between the reference and observed signals, clearly showing an optimal range of 3.75 m and an optimal velocity of 0.31 m/s (Martinez, A., & Marchand, J. L. , 1993). Finally, the system's performance in detecting high-resolution targets is analyzed, and practical challenges, such as periodic spurious peaks and signal processing complexities, are examined. Finally, this simulation method allows the study of system capabilities without the need for field tests.

## FINDINGS

This research investigates the use of fifth-generation (5G) mobile network signals as illuminator sources in semi-active radar (SAR). Simulation findings show that despite the main challenges, such as strong direct signal and multipath signals that obscure the target, these obstacles can be suppressed by using an adaptive filter based on the least mean squares (LMS) algorithm (Rai et al., 2021) The results of the simulation of a single target with a two-way range of 120 m and a speed of 40 km/h showed that before filtering, the target was almost impossible to identify due to substantial interference. However, after applying the adaptive filter, the target was clearly distinguishable in the range-Doppler plane. In a second scenario with two targets close together (range 160 and 165 m and speed 38 and 36 km/h), the system succeeded in separating and detecting both targets after filtering, which demonstrates the good range resolution and speed capability of the 5G-based PARS system (Wang et al., 2020).

However, a challenge was identified: the appearance of repetitive spurious peaks with a two-way speed interval of about 11.13 km/h, which is caused by the periodic structure of the 5G signal with a period of 10 milliseconds. These peaks are more noticeable in conditions where the demand for network resources is low and many signal symbols remain empty. In case of a busy signal (high network traffic), the level of these spurious peaks is significantly reduced, although the signal processing becomes more complex. This study demonstrates the effectiveness of using 5G signals and a simple LMS algorithm for semi-active radar in an urban scenario. This research investigated the effectiveness of semi-active radar (PARS) using 5G signals. Key findings show that the strong direct and multipath signal obscures the target, but a simple adaptive filter (LMS) can effectively suppress this interference. Simulations confirmed the system's ability to detect and separate closely spaced targets after

filtering. One challenge identified was the repetitive spurious peaks caused by the periodic structure of the 5G signal, the intensity of which depends on the network load. Overall, this study demonstrates the potential of using existing 5G signals for surveillance applications in urban environments (Nascimento & Silva, 2014)

### Communication Signals 5G

5G signals refer to the radio waves and digital protocols used to transmit data in fifth-generation (5G) mobile networks. These signals are designed using advanced technologies that enable higher speeds, lower latency, and the simultaneous connection of more devices. 5G technology is based on OFDM (Orthogonal Frequency Division Multiplexing), which can reduce interference by distributing a digital signal across multiple channels. 5G uses the 5G NR (New Radio) air interface along with OFDM principles and leverages wider bandwidth technologies, such as the gigahertz range (Ramraj, D., Praveen, L., & Giovanni, P., 2022). The frequency resource of 5G mobile networks is divided into 2 frequency ranges (Veremyev, V., & Kutuzov, M., 2024). The first frequency range (FR1) includes frequencies below 6 GHz, the second (FR2) – from 24.25 to 71.0 GHz. the maximum bandwidth in FR1 is 100 MHz, in FR2 – 400 MHz.

At the end of January 2024, the Russian government adopted a decision to allocate the frequency range from 4.4 to 4.99 GHz for the operation of 5G networks in Russia. According to the technical specifications of the fifth generation standard in the 3G project, the range 4.4 ... 4.99 GHz belongs to the n79 band (4.4 ... 5 GHz). In Table. 1 shows the parameters of the n79 band signal (Qisong et al., 2011).

**Table 1.** Numerology for 5G signal in n79

| $\mu$ | $\Delta f_c$<br>KHz | Bandwidth,<br>MHz                       | $N_{sl}$ | $N_{sim}$ | Cyclic prefix      |
|-------|---------------------|---|----------|-----------|--------------------|
| 0     | 15                  | 10, 20, 30, 40, 50                      | 1        | 14        | Normal             |
| 1     | 30                  | 10, 20, 30, 40, 50, 60, 70, 80, 90, 100 | 2        | 14        | Normal             |
| 2     | 60                  | 10, 20, 30, 40, 50, 60, 70, 80, 90, 100 | 4        | 14 or 12  | Normal or extended |

Transmission in 5G networks is based on cyclic prefix orthogonal frequency division multiplexing (CP-OFDM). Unlike LTE signals that only support one type of subcarrier spacing, with  $\Delta f_c = 15 \text{ KHz}$ , 5G it uses subcarriers with different spectrum widths (Generation Partnership Project (3GPP)., 2021). The 5G signal carriers depend on numerology, which is determined by the parameter  $\mu \in \{0, 1, 2, 3, 4, \}$  and with the formula  $\Delta f_c = 2^\mu \cdot 15$  it is determined. 5G signal sources are distributed in the time and frequency domains. In the time domain, the 5G signal is measured in frames. A frame is 10 milliseconds long and consists of 10 sub-frames of 1 millisecond length (Okoń, M., & Kawalec, A., 2016). Each sub-frame is divided into slots, the number of which is  $N_{sl} = 2^\mu$ . Depending on the type of cyclic prefix, a slot consists of 14 or 12 characters. A symbol is the most minor time interval in the time domain, and in the frequency domain, it is the smallest frequency quantum of a subcarrier. A resource element is the smallest time-frequency resource consisting of a symbol and subcarrier (Ramraj et al., 2022).

A resource block is defined only in the frequency domain and consists of 12 subcarriers. All the existing resource blocks form what is called a resource network. Resources are assigned to several channels and signals. This article focuses on the following physical signals and channels:

- Primary Synchronization Signal (PSS) - A primary synchronization signal that allows user devices to synchronize in frequency and time.
- Secondary Synchronization Signal (SSS) - Secondary synchronization signal used to determine the physical identity of a cell.
- Physical Broadcast Channel (PBCH) - Physical broadcast channel for transmitting system information to user devices during cell search.
- Physical Downlink Control Channel (PDCCH) – A downlink physical control channel for transmitting control information from the base station to the user device.
- Physical Downlink Shared Channel (PDSCH) – Physical downlink shared channel for transmitting user data from the base station to the user device.
- Demodulation Reference Signal (DM-RS) - A demodulation reference signal that allows user devices to perform channel estimation and demodulation of associated physical channels.
- Phase Tracking Reference Signal (PT-RS) - A reference tracking signal that allows one to evaluate and minimize the impact of overall phase error on system performance.
- Channel State Information Reference Signal (CSI-RS) - A reference signal containing information about the channel state, allowing one to evaluate the channel and provide information about its quality (Reigber, A. , 2013).
- Each of these channels/signals has a different purpose, is located in different places in the time-frequency network, and is encoded differently (3rd Generation Partnership Project (3GPP). , 2021).

### **Semi-Active Radar Scenario**

A typical radar scenario for 5G-based PARS is shown in Figure 1. The 5G base station acts as an illumination source for the entire radar scene. The PARLS receiving position consists of two data collection channels: a reference channel and an observation channel. The reference channel is used to receive the primary transmitted signal. This is achieved by pointing the antenna towards the transmitter (Rai et al., 2021). The other antenna faces the observation area of the desired target, and the channel is the receiving signal echo. The mathematical relationship of the reference channel signal is:

$$S_{straight}(t) = A_0 x(t - \tau_0) + \omega_{straight}(t).$$

Where  $A_0$  - is the complex amplitude of the direct signal at a delay time  $\tau_0$  in the reference channel;  $x(t)$  - the signal transmitted from the backlight source;  $\omega_{straight}(t)$  - noise in the reference channel (Okoń & Kawalec, 2016).

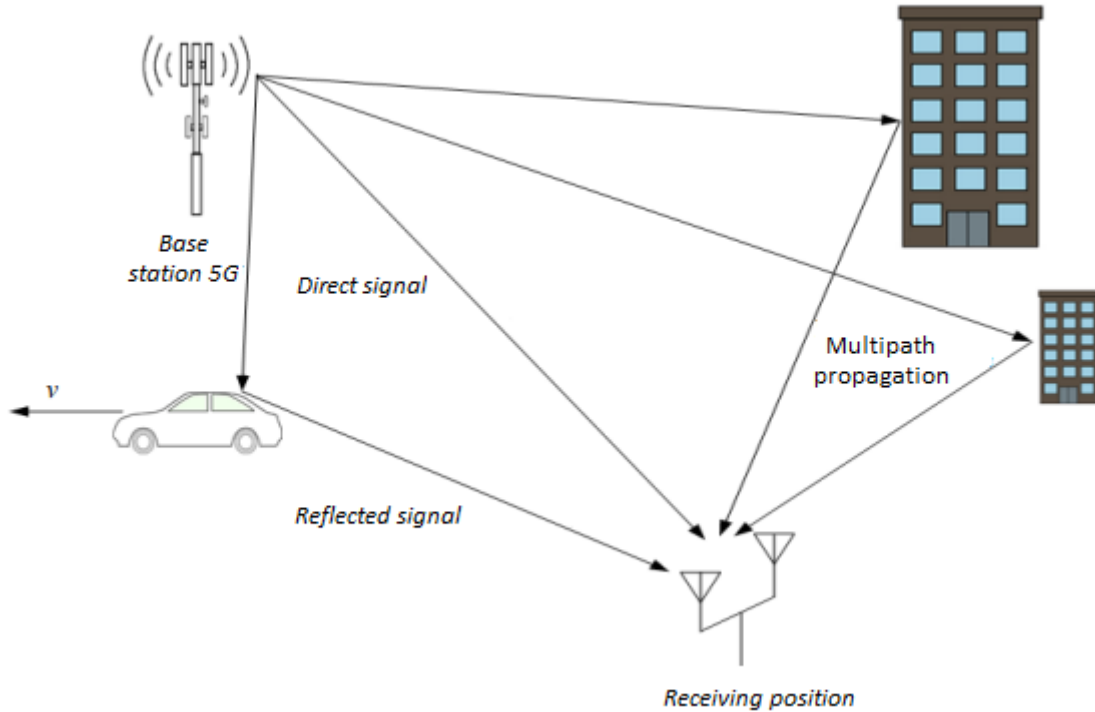


**Figure 1.** Passive radar scenario (Aleksey, B., & Evgenij, V. , 2016).

In Figure 1, the observation channel signal consists of four parts. The first is the straight tracking signal  $S_{straight}(t)$ ; the second is the echo signals reflected from the targets  $S_{echo}(t)$ ; the third is the signals determined by multipath propagation and reflected from stationary objects in the background  $S_{many}(t)$ ; and the last is the noise signal in the observation channel  $\omega_{nab}(t)$ . Then the general expression for the received signal is (Blázquez, R., Ummenhofer, M., & Cristallini, D. , 2022).

$$S_{nab}(t) = S_{straight}(t) + S_{echo}(t) + S_{many}(t) + \omega_{nab}(t).$$

Or

$$S_{nab}(t) = Ax(t - \tau_0) + \sum_{m=1}^M A_m x(t - \tau_m) + \sum_{k=1}^K A_k x(t - \tau_k) e^{j2\pi f_{dk}t} + \omega_{nab}(t).$$

Where  $A$  - is the complex amplitude of the direct signal in the observation channel;  $M$  - is the number of stationary interference sources;  $A_m$  - is the complex amplitude of stationary interference;  $K$  - is the number of target sources;  $A_k$  - is the complex amplitude of the received signal from the  $k$ -th target with a delay  $\tau_k$ ;  $f_{dk}$  - is the Doppler shift of the  $k$ -th target;  $\omega_{nab}(t)$  - is the noise in the observation channel (Charvat, L., & Kempel, C. , 2006).

At the receiving position, the mutual uncertainty function (MUF) of the signals in the observation and direct path channels is calculated to determine the bistatic range and target velocity (Aleksey, B., & Evgenii, V. , 2016).

$$\chi(\tau, f_d) = \int_{-\infty}^{\infty} S_{nab}(t) S_{straight}^*(t - \tau) e^{-j2f_d t} dt.$$

Often, the strength of the direct signal, signals due to multipath propagation, and interference are much higher than the target signal, which leads to the masking of echo signals from a moving target. Hence, the method of their suppression is essential for the performance of PARS. The sum of many  $S_{straight}(t) + S_{many}(t)$  Represents an unwanted component, the level of which must be minimized by noise filtering methods. To suppress the influence of interfering signals due to direct and multipath propagation in the observation channel, an adaptive filter is used. The most common adaptive filters are: the least mean square (LMS) method; normalized least squares (NLMS); recursive least squares (RLS) (Martinez, A., & Marchand, J. L. , 1993). The extended cancellation algorithm (ECA) and the RMS lattice filter (Last Square Lattice – LSL). Each of the algorithms has its own characteristics. In the described work, an LMS-based algorithm is used to suppress interference. The LMS algorithm has the following advantages over other methods (Griffiths H. D. & Baker, 2017): simplicity of calculation, ease of use, and high reliability.

*The least squares method (LMS)* is the most widely used adaptive filter algorithm in practice. It is designed to simulate the desired filter by finding its coefficients, which are related to obtaining the minimum mean square of the error signal (Farhang-Boroujeny, 2013).

The least squares filter algorithm is divided into two main processes - filtering and adaptation (Nascimento V. H., 2014). The filtering process involves two primary operations: calculating the filter output using the discrete input signal and the error signal, which is the difference between the desired response and the filter output (Nascimento V. H., 2014).

The discrete output signal of the LMS filter can be described as follows:

$$y(k) = \sum_{n=0}^N \mathcal{W}_n x(k - n)$$

Where  $\mathcal{W}$  - the adaptive coefficient of the filter, and  $x(k)$  - the input discrete signal. is the error signal

$$e(k) = d(k) - \sum_{n=0}^N \mathcal{W}_n x(k - n) = d(k) - \mathbf{x}^T(k) \mathbf{W},$$

Where  $d(k)$ - reference signal,  $d(k)$  And  $\mathbf{W}$  - column vectors.

During the adaptation process, the filter weight is adjusted using the error estimated during the filtering process.

The following expression determines the filter weight

$$W(k+1) = W(k) + \mu x(k)e(k).$$

Where  $\mu$  - is a positive coefficient (step size).

Typically, the time delay and Doppler shift values of a target in a PARS are estimated by detecting the EFF peaks between the reference signal and the residual signal (i.e., the adaptive filter error signal) that contains the target echo signal of interest after clutter suppression. The discrete-time expression of VFN is defined as

$$\chi(l, P) = \sum_{i=0}^{M-1} S_e(i) S_{support}^*(i-l) e^{-\frac{j2\pi p_i}{M}}.$$

Where ( $l = 0, \dots, R-1$ ) - range element number (delay);  $R$  - number of range elements; ( $P = -P, -P+1, \dots, P-1, P$ ) - Doppler channel number;  $(2P+1)$  - number of Doppler channels (Cheng, P., & Wan, J., 2015).

**Simulation Parameters:** Current user needs are the basis for the allocation of frequency-time resources by the network scheduler.

Depending on the level of demand for resources, the scheduler may use all of them when the load is very high and almost none (except for the synchronization signal) when the load is low. This simulation considers a scenario in which a 5G user device is connected to a base station serving the communication segment and constantly exchanges data with it. It is assumed that the 5G signal operates in Time Division Duplex (TDD) mode. The technical parameters of the 5G signal used in the simulation are given in Table 2.

Fig. 2 shows the 5G downlink signal for one user in the time domain (Nascimento V. H., 2014).

In practice, the process of signal processing in PARLS should perform the reference signal recovery procedure. The relationship between the signals and channels of the 5G downlink signal, as well as the process of reference signal recovery, is expected to be considered in more detail in subsequent studies (Feifeng, L., Cheng, H., & Teng L., 2010).

**Table2.** Parameters for modeling 5G downlink signal

| Parameter  | Value   |
|--|---|
| Channels and signals                                 | PSS, SSS, PBCH, PDCCH, PDSCH, DM-RS                       |
| Center frequency, MHz                                | 4850  |
| Bandwidth ( $\Delta f_0$ ), MHz                      | 40  |
| Subcarrier interval, kHz                             | PSS, SSS, and PBCH: 30,<br>other channels and signals: 15 |
| Accumulation time ( $T_c$ ), ms                      | 100   |
| Sampling frequency, MHz                              | 61.44   |
| Repetition period ( $T_b$ ), ms                      | 10  |
| Signal-to-noise ratio in the observation channel, dB | 20  |
| Signal-to-noise ratio in the reference channel, dB   | 100   |



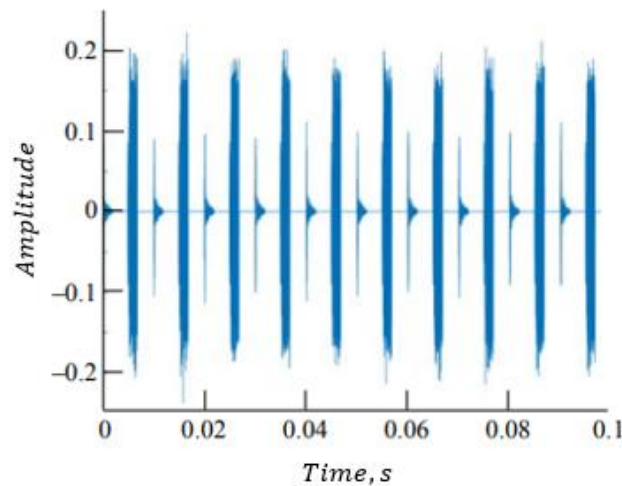


Fig. 2. 5G Signal for one user in the time domain (3rd Generation Partnership Project (3GPP)., 2020)

When modeling the unwanted components in the observation channel, the technique presented in (Veremyev, V., & Kutuzov, M., 2024). was used. This document describes a method for modeling, designing, optimizing, and evaluating 5G systems defined by 3GPP. The channel model can be used for both channel and system-level modeling under various conditions. For example, scenarios such as urban macro cell, indoor office, rural macro cell, and indoor factory are supported for system-level modeling. Meanwhile, it is possible to simulate the 5G signal propagation in each of the system level scenarios, both Line of Sight (LOS) and Non Line of Sight (NLOS), etc etc (3rd Generation Partnership Project (3GPP)., 2020).

Two stochastic channel models are defined to estimate the communication parameters between a 5G base station and user devices in different scenarios: Clustered Delay Line (CDL) and Tapped Delay Line (TDL). Each cluster in the CDL channel model contains multipath components with the same delay but with minor differences in the emission and reception angles (Charvat, L., & Kempel, C., 2006). TDL is a simplified channel model used in modeling the physical layer of mobile communication systems, excluding the spatial coding method of the signal (multiple-input and multiple-output - MIMO). Instead of using the general models available in the standards, this paper proposes a new channel model for the urban macrocell - line-of-sight scenario according to the rules defined in (3rd Generation Partnership Project (3GPP)., 2021) .

Multipath propagation results in different delays, which can be obtained randomly from the delay distribution in the channel model.

$$\tau'_n = -r_\tau \Delta\tau \ln X_n.$$

Where  $r_\tau$  – is the coefficient of proportionality of the delay distribution;  $\Delta\tau$  is the delay spread, which occurs due to multipath propagation [15];  $X_n$  – is a random variable with a uniform distribution over (0, 1).

During the modeling process, the delay is normalized, the minimum delay is subtracted, and they are sorted in ascending order:

$$\tau_n = \text{variety}(\tau'_n - \min(\tau'_n)).$$

For the LOS condition, the delay is:

$$\tau_n^{LOS} = \frac{\tau_n}{0.775 - 0.0433k + 0.0002k^2 + 0.000017k^3}.$$

The cluster power is calculated as

$$P'_n = \exp\left(-\tau_n \frac{r_\tau - 1}{r_\tau \Delta\tau}\right) 10^{\frac{-Z_n}{10}}.$$

Where  $Z_n \sim N(0, \xi^2)$ - is the shading coefficient for each cluster, dB.

The cluster power is normalized as follows:

$$P_n = \frac{P'_n}{\sum_{n=1}^N P'_n}$$

For the LOS condition, an additional mirror component is added to the first cluster, and the cluster cardinality is defined as

$$P_n = \frac{1}{K_R + 1} \frac{P'_n}{\sum_{n=1}^N P'_n} + \delta(n - 1) \frac{K_R}{K_R + 1}$$

Where  $K_R$  is the Rice  $K$ -factor transformed into a linear scale;  $\delta(\cdot)$  is the delta function.

Table 3 presents the calculated parameters of the developed channel model, which are further used in modeling the multipath scenario in *PARLS*.

**Table 3.** Channel model parameters

| number | Delay, Nsec | Power, dB |
|--------|-------------|-----------|
| 1      | 0           | -0.2      |
| 2      | 210         | -19.1     |
| 3      | 215         | -15.9     |
| 4      | 805         | -24.2     |
| 5      | 1050        | -21.1     |
| 6      | 2075        | -24.9     |

To filter out noise during modeling, an adaptive *LMS* filter with a step size of 0.01 and a filter length of  $M = 64$  is used (Veremyev, V., & Kutuzov, M., 2024).

**Simulation.** Since simulation is the process of representing the characteristics of a system through the use of conventional parameters and computer programs based on a design (Zhenyu, H., Yang, Y., & Duoje, W., 2022). as shown in Figure 3, Two scenarios for an urban macrocell are considered, in which a hypothetical target is located in a coverage area of up to 650 m and has a speed of less than 60 km/h. For the given 5G signal parameters (Table 2) the best range resolution is 3.75 m ( $\Delta R = c / 2\Delta f_0$ ), and the best radial velocity resolution is 0.31 m/sec ( $\Delta v_r = \lambda / 2T_c$ ) In the first scenario, a single target was simulated

with bistatic range values  $R_b = 120 \text{ m}$  and velocity  $\mathcal{V}_b = 40 \text{ km/h}$ . The simulation results are shown in Fig. 3.

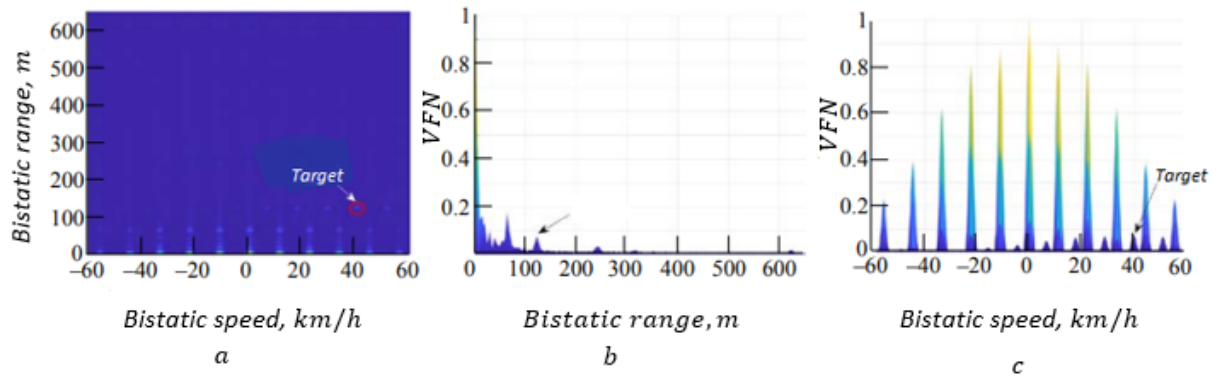


**Fig. 3.** CAF before adaptive filtering for the first scenario: *a* – the range–Doppler plane; *b* – the range cross-section; *c* – the velocity cross-section (Cheng, P., & Wan, J., 2015)

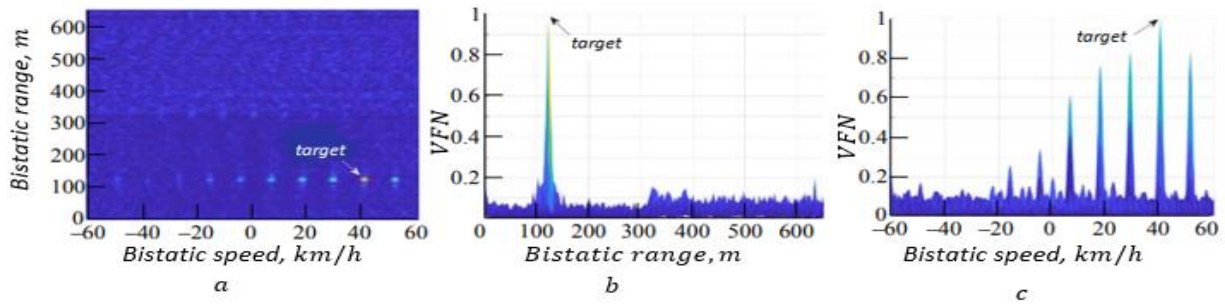


**Fig. 4.** CAF after adaptive filtering for the first scenario: *a* – the range plane; *b* – the range cross-section. *c* – The velocity cross-section (Cheng, P., & Wan, J., 2015).

From Fig. 3*a*, it can be seen that before adaptive filtering, target detection is difficult due to substantial interference and multipath propagation. The most prominent peak in the range-Doppler plane corresponds to the direct signal in the observation channel. The target mark differs from other marks by the Doppler shift. In contrast, the target is well detected after adaptive filtering, as shown in Fig. 4*a*.

In Fig. 3, *a*, *c*, and 4, *a*, *c*, the appearance of an undesirable series of false peaks is visible. At a carrier frequency of  $4850 \text{ MHz}$ , the downlink 5G signal for one user is repeated with a period of  $T_b = 10 \text{ ms}$  (see Fig. 2), and the false peaks are repeated with an interval of the bistatic rate

$$v_L = \frac{\lambda}{2T_b} \approx 3.093 \text{ m/sec}(11.13 \text{ Km/hr}).$$

In case of high demand for 5G resources (i.e., a large number of users), the 5G downlink signal is filled in almost all symbols, which leads to a significant decrease in the false peak level. However, accordingly, the process of processing the 5G downlink signal becomes algorithmically more complex (Young S., 2015).

The second scenario is a hypothetical situation to demonstrate the range and velocity resolution of PARLS using a 5G signal. Two targets have close bistatic range and velocity, respectively.  $R_{b1} = 160 \text{ m}$ ;  $v_{b1} = 38 \text{ km/h}$  and  $R_{b2} = 165 \text{ m}$ ;  $v_{b2} = 36 \text{ km/h}$ . The simulation results of the second scenario after adaptive filtering are shown in Fig. 5.

From Fig. 5, it can be seen that the marks of the two targets are located close to each other, but can be clearly distinguished (Du et al., 2010).

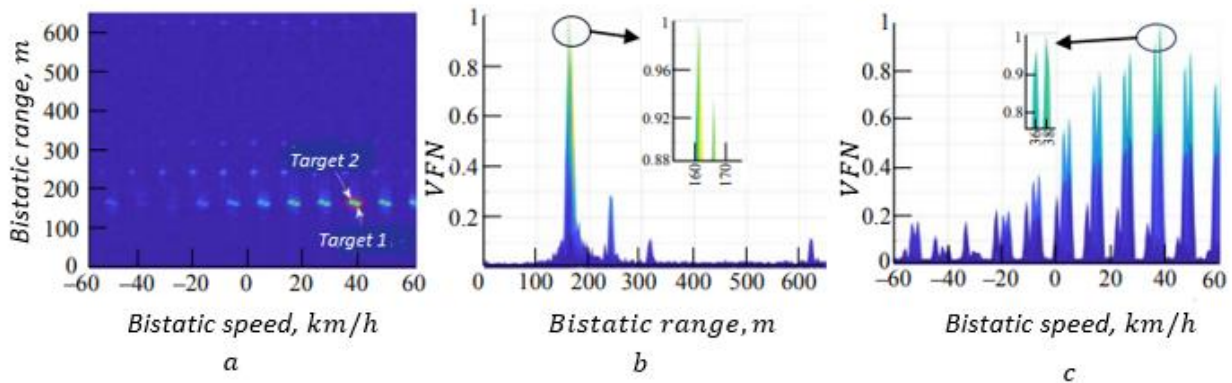


Fig. 5. CAF in the second scenario: a – range-Doppler plane; b – range cross section; c – velocity cross section (Cheng, P., & Wan, J., 2015)

## DISCUSSION

The findings of this simulation-based study directly address the research questions and objectives, demonstrating both the significant potential and operational complexities of integrating 5G signals into semi-active radar systems (PARLS) (Brooker, G., 2011). The simulation results clearly demonstrate that the high bandwidth (40 MHz in the n79 band) inherent in 5G signals is a key factor in achieving high range resolution (Veremyev & Kutuzov, 2024). The theoretical range resolution of 3.75 is calculated as ( $\Delta R = c / 2\Delta f_0$ ), which was experimentally confirmed in the second scenario (detecting two targets only 5 m apart), is evidence of this claim (Cheng & Wan, 2019). Furthermore, the 5G signal structure, especially the synchronization signals (PSS, SSS), enables precise time-frequency synchronization, which is crucial for calculating the target velocity (3rd Generation Partnership Project (3GPP), 2021). These results clearly demonstrate that 5G technology has tangible advantages over traditional illumination sources and opens up new opportunities for high-resolution applications (Gomez & Samczynski, 2022).

Regarding the challenges, this study identified two main obstacles:

1. Strong interference: the very high power of the direct signal and the multipath clutter ( $S_{straight}(t) + S_{many}(t)$ ) Completely mask the target echoes (Fig. 3a). However, effective suppression of these components using a relatively simple LMS adaptive filter shows that this challenge is not insurmountable and can be overcome with standard signal processing techniques (Figure 4a) (Rai et al., 2021).

2. Signal-induced ambiguities: A unique and significant challenge identified is the appearance of periodic spurious peaks at two-base speed intervals of approximately 11.13 km/h ( $v_L = \lambda/2T_b$ ). This phenomenon is a direct consequence of the periodic structure of the 5G signal with a periodic period of 10 milliseconds ( $T_b$ ) (Figure 2) (3rd Generation Partnership Project (3GPP). , 2021). This finding, which is not common in traditional radar waveforms, demonstrates a deep understanding of the trade-off between useful signal structure and unwanted ambiguities, and suggests that for optimal performance in real-world conditions (with low network load), more advanced processing algorithms than the basic LMS may be required (Martelli et al., 2021).

This study clearly goes a step further than previous research:

From theory to practice: Instead of discussing general principles, it focuses on a specific implementation (band n79 in Russia) (Veremyev, V., & Kutuzov, M. , 2024).

From general to specific: Instead of using standard channel models (such as CDL/TDL), it presents a new channel model suitable for urban environments (3rd Generation Partnership Project [3GPP], 2020).

From description to demonstration: Instead of listing possible methods, an algorithm (LMS) is chosen and its efficiency is demonstrated by simulation and illustrated results (Figures 3, 4, and 5) (Nascimento & Silva, 2014)

Discovering new challenges: In addition to demonstrating successes, a new challenge (periodic spurious peaks) is identified and analyzed, which is crucial for the future development of this technology. In summary, this research demonstrates the tremendous potential of 5G signals as a passive illumination source for high-resolution surveillance applications in urban environments (Blázquez-García, R., & Markiton, P. , 2024). However, to realize this potential in the real world, the identified operational challenges must be overcome, particularly the effects of the signal's periodic structure and the dependence of performance on network load. This requires the development of more innovative processing algorithms and extensive experimental studies with the deployment of 5G networks, as also emphasized in the recommendations section of the paper (Reigber, 2013).

As a result, the present study and previous studies presented in the discussion section can be separated and compared as follows:

| Feature          | Current Study   | Previous Studies  |
|------------------|---|---|
| Key findings     | Detection of periodic spurious peaks due to 5G frame structure                | Identifying general challenges such as frequency interference and processing complexity |
| Method of proof  | Simulation and presentation of illustrated results (Figures 3, 4, 5)          | Mainly theory and suggestions for the future  |
| Scope of focus   | Specific: n79 band and a new urban channel model                              | General: Discussing the potential of 5G in general                                      |
| Type of analysis | Proof of the effectiveness of a simple algorithm (LMS) and trade-off analysis | Suggesting the use of complex algorithms (ML, Super-resolution)                         |
| Conclusion       | Focus on practical challenges and implementation barriers                     | Focusing on future opportunities and applications                                       |

## **CONCLUSION**

This paper analyzed the downlink signals and channels in the 5G communication system in the n79 range. It was demonstrated that the simulation of the 5G signal processing process, used as illumination in PARLS, was still performed, analyzing the VFN calculation results for two radar scenarios. The simulation results show that the PARLS using the 5G signal is capable of detecting targets with good resolution in both range and speed. The simulation results further confirm the possibility of effectively using 5G communication signals in PARLS as illumination for the purpose of monitoring the situation in relatively small areas. Meanwhile, semi-active radar, which utilizes external illumination sources, is one of the most active areas of research and development in the field of creating air and maritime surveillance systems. It has made significant efforts to improve the underlying processing algorithms, focusing on minimizing computational complexity and achieving efficiency.

In addition, as research continues to utilize new emerging signal sources in the development of new semi-active radar systems (PARLS), the development of 5G networks has provided new illumination sources for semi-active radars. According to previous evaluations and studies, PARLS has demonstrated that using 5G signals with relatively limited coverage and operational area, it achieves high quality in terms of range and speed. PARLS using 5G signals could be used for vehicle monitoring, mainly to ensure safety in rail transport or at intersections.

On the other hand, the structure and main characteristics of the 5G signal were examined in two cases. Modeling was carried out for two possible radar scenarios. With one and two moving targets in a multi-beam environment, and the modeling results were analyzed. Nowadays, most of the technologies considered for imaging the surrounding environment have overcome the obstacles of semi-active radar sensors. The number of semi-active radars in applications such as automotive is increasing, which causes spectrum sharing and interference between radars operating in the same band. This problem can be solved in the future by using semi-active radar technology, especially the 5G-based concept presented in this paper. The proposed concept may be a game changer in future sensing applications in dense urban areas, where significant vehicle traffic poses a bigger problem for the larger number of semi-active radars that may interfere with each other.

## **Recommendations**

Given the broad applicability of the topic and its relevance to new findings, the authors suggest that more research results be reviewed in the relevant section. Secondly, the parameters involved in the research results, such as the study area, frequency range, effective modeling methods, sensor obstacle detection, data collection in the environment for practical experiments, application of different algorithms for information extraction and data analysis, should be carefully and adequately considered.

Finally, the retrieval of the reference signal from the complex 5G signal is a crucial and challenging next step that requires careful investigation, as the success of the above

suggestions can significantly enhance the accuracy and reliability of the 5G-based passive radar system.

1. The authors were responsible for the “generation” of the raw data by writing the simulation codes.
2. Seyyed Sarwar Ebtekar and Rajab Ali Khavari carried out conceptualization and supervision of the study.
3. The data were computationally generated by the authors (Seyed Sarwar Ebtekar and Rajab Ali Khavari) rather than collected through experimental means.

## **FUNDING INFORMATION**

No funding is available for the manuscript.

## **CONFLICT OF INTEREST STATEMENT**

The authors of this article have no conflicts of interest (financial, professional, or personal) that could influence the results or interpretations of this research.

## **DATA AVAILABILITY STATEMENT**

All data generated or analysed during this study are included in this published article and its supplementary information files (Tables 1, Tables 2 & Tables 3).

## **REFERENCES**

- Aleksey, B., & Evgenii, V. (2016). Passivnaya kogerentnaya radiolokaciya [Passive coherent radar]. *Journal of Communications Technology and Electronics*, 27(1), 67–78. <https://doi.org/10.32603/1993-8985-2024-27-1-67-78>
- Blázquez, R., Ummenhofer, M., & Cristallini, D. (2022). Passive radar architecture based on broadband LEO communication satellite constellations. *2022 IEEE Radar Conference (RadarConf22)*, 1–6. <https://doi.org/10.1109/RadarConf2248738.2022.9764342>
- Blázquez-García, R., & Markiton, P. (2024). Passive radar imaging based on multistatic combination of Starlink and OneWeb illumination. *2024 IEEE Radar Conference (RadarConf24)*, 1–6. <https://doi.org/10.1109/RadarConf2458775.2024.10548646>
- Brooker, G. (2011). *Introduction to sensors for ranging and imaging*. SciTech Publishing. <https://doi.org/10.1049/SBRA014E>
- Cafforio, C., Prati, C., & Rocca, F. (1991). SAR data focusing using seismic migration techniques, 27(2), p. 194 – 207. <https://doi.org/10.1109/7.78293>.
- Carrara-Walter, G., & Majewski-Ronald, M. (1995). Spotlight synthetic aperture radar : signal processing algorithms. [Link](#)
- Charvat, G. (2007). *A low-power radar imaging system* (2nd ed.) [Master's thesis, Michigan State University]. ResearchGate. [Link](#)

- Charvat, L., & Kempel, C. (2006). Synthetic aperture radar imaging using a unique approach to frequency modulated continuous-wave radar design, vol. 48, no. 1, <https://doi.org/10.1109/map.2006.1645606>.
- Cheng, P., & Wan, J. (2015). Refocusing of ground moving targets for range migration algorithm in FMCW SAR 2015, vol. 9642. <https://doi.org/10.1117/12.2194246>.
- Du, L., Wang, Y., & Wu, Y. (2010). A Three Dimensional Range Migration Algorithm for Downward-Looking 3D-SAR with Single-Transmitting and Multiple-Receiving Linear Array Antennas. *EURASIP J. Adv.* <https://doi.org/10.1155/2010/957916>.
- Farhang, B. (2013). Adaptive filters theory and applications. Chichester, West Sussex, United Kingdom, John Wiley. [Link](#)
- Feifeng, L., Cheng, H., & Teng L. (2010) A novel Range Migration Algorithm of GEO SAR echo data, in (IGARSS). <https://doi.org/10.1109/IGARSS.2010.5651127>.
- Gomez, H., & Samczynski, P. (2022). The STARLINK-based passive radar: Preliminary study and first illuminator signal measurements. *23rd International Radar Symposium (IRS)*, Gdansk, Poland. <https://doi.org/10.23919/IRS54158.2022.9905046>
- Gómez, M., & Mata-Moya, D. (2020). DVB-T receiver independent of channel allocation, with frequency offset compensation for improving resolution in low cost passive radar. *IEEE Sensors Journal*, 20(24). <https://doi.org/10.1109/JSEN.2020.3011129>
- Griffiths, H. D., & Baker, C. J. (2017). *An introduction to passive radar*. [Book]. [Link](#)
- Martelli, T., Cabrera, O., & Colon, F. (2020). Lombardo P. Exploitation of Long Coherent Integration Times to Improve Drone Detection in DVB-S based Passive Radar. *IEEE Radar Conf. (RadarConf20)*, Florence. <https://doi.org/10.1109/RadarConf2043947.2020.9266624>.
- Martinez, A., & Marchand, J. L. (1993). SAR image quality assessment, *Rev. Teledetec.*, vol. 2, [Link](#)
- Nascimento, H., & Silva M. T. (2014). Adaptive Filters. Academic Press Library in Signal Processing, vol. 1. <https://doi.org/10.1016/B978-0-12-396502-8.00012-7>.
- Okóń, M., & Kawalec, A. (2016). An analysis of Chosen Image Formation Algorithms for Synthetic Aperture Radar with FMCW. [Link](#)
- Qisong, W., Liang, Y., & Mengdao, X. (2011). Focusing of tandem bistatic-configuration data with range migration algorithm. vol. 8. P, 88-92. <https://doi.org/10.1155/2016/3251082>.
- Rai, P. K., Kumar, A., & Khan, M. Z. (2021). LTE-Based Passive Radars and Applications: A Review. Vol, 42. <https://doi.org/10.1080/01431161.2021.1959669>
- Ramraj, D., Praveen, L., & Giovanni, P. (2022). Investigation on 5G Technology: A Systematic Review. <https://doi.org/10.3390/s22010026>.



- Reigber, A. (2013). Very-high-resolution airborne synthetic aperture radar imaging: Signal processing and applications. *Proceedings of the IEEE*, 101(3). <https://doi.org/10.1109/jproc.2012.2220511>
- Veremyev, V., & Kutuzov, M. (2024). Feasibility study of using 5G signals for illumination purposes in passive radar. *Radiophysics and Quantum Electronics*, 27(1), 67–78. <https://doi.org/10.32603/1993-8985-2024-27-1-67-78>
- Wang, R., Loffeld, O., & Knedlik, M. (2010). Focus FMCW SAR data using the wavenumber domain algorithm. *IEEE Transactions on Geoscience and Remote Sensing*, 48(4). <https://doi.org/10.1109/TGRS.2009.2034368>
- Xin, L., & Hong, S. (2007). Parameter assessment for SAR image quality evaluation system. *Proceedings of the Asian and Pacific Conference on Synthetic Aperture Radar (APSAR)*. <https://doi.org/10.1109/APSAR.2007.4418554>
- Young, O. (2015). Focusing bistatic FMCW SAR signal by range migration algorithm based on Fresnel approximation. *Sensors*, 15(12), 29910–29925. <https://doi.org/10.3390/s151229910>
- Zhenyu, H., Yang, Y., & Duojie, W. (2022). Range resolution improvement of GNSS-based passive radar via incremental Wiener filter. *IEEE Geoscience and Remote Sensing Letters*, 19. <https://doi.org/10.1109/LGRS.2021.3130062>
- 3rd Generation Partnership Project (3GPP). (2020, November). *Study on channel model for frequencies from 0.5 to 100 GHz* (3GPP TR 38.901 version 16.1.0 Release 16). European Telecommunications Standards Institute (ETSI). [Link](#)
- 3rd Generation Partnership Project (3GPP). (2021, August). *5G; Physical channels and modulation* (3GPP TS 38.211 version 16.6.0 Release 16). European Telecommunications Standards Institute (ETSI). [Link](#)
- 3rd Generation Partnership Project (3GPP). (2021, January). *5G; NR; Base station (BS) radio transmission and reception* (3GPP TS 38.104 version 16.6.0 Release 16). European Telecommunications Standards Institute (ETSI). [Link](#)